ACADEMIC PRESS

Available online at www.sciencedirect.com
SCIENCE DIRECT®

Journal of Catalysis 219 (2003) 197–205

JOURNAL OF CATALYSIS

www.elsevier.com/locate/jcat

Comparative studies of the N_2O/H_2, N_2O/CO, H_2/O_2 and CO/O_2 reactions on supported gold catalysts: effect of the addition of various oxides

A.C. Gluhoi,[a] M.A.P. Dekkers,[b] and B.E. Nieuwenhuys [a,*]

[a] *Leiden Institute of Chemistry, Department of Heterogeneous Catalysis and Surface Chemistry, PO Box 9502, 2300 RA Leiden, The Netherlands*
[b] *Fluor Daniel BV, PO Box 4354, 2003 EJ Haarlem, The Netherlands*

Received 23 December 2002; revised 31 March 2003; accepted 8 April 2003

Abstract

The reduction of N_2O with H_2 and CO has been investigated on Au/TiO_2, Au/Al_2O_3, $Au/M^IO_x/M^{II}O_x/Al_2O_3$, and $Au/MO_x/Al_2O_3$ (M^I, M^{II}, M = Li, Rb, Mg, Co, Mn, Ce, La, Ti). In addition, for comparison, the oxidation reactions of H_2 and CO with O_2 have been studied on some selected catalysts. All the samples are highly active at low temperatures for all the reactions. The oxides added to Au/Al_2O_3 improve the catalytic performance of gold. Interesting and synergistic effects were observed when a mixture of metal oxides is added to Au/Al_2O_3, e.g., Rb_2O (Li_2O) and CeO_x. Possible mechanisms are proposed.

Keywords: Gold; Nitrous oxide; Carbon monoxide; Hydrogen; Oxygen; Additives; Transition metal oxides; Alkali metal oxides

1. Introduction

The great interest in gold catalysis in the last years [1–3] is due to the recently found high catalytic activity of gold-based catalysts for a number of important reactions such as CO oxidation [2,4,5], WGS reaction [6,7], and hydrogenation of unsaturated hydrocarbons [8,9]. Various factors can influence the catalytic activity of gold-supported catalysts and the most important ones are: (a) the gold particle size which must be in the nanometer range [3,10], and (b) the nature of the support or additives. Many studies demonstrated that gold becomes very active if it is supported on, or promoted by, transition-metal oxides [3,11–15]. In view of the more stringent legislation regarding NO_x emission from vehicles, gold-based catalysts were also tested for NO reduction by propene in the presence of oxygen [16], by H_2 [17–19], and by CO [20]. Nitrous oxide is a principal product of NO reduction and is regarded as an undesired and harmful gas in automotive exhaust gases. There are not many papers dealing with N_2O decomposition and reduction on gold catalysts. However, the few available data show that Au/TiO_2 and $Au/CoO_x/TiO_2$ are promising catalysts for CO/N_2O reaction [21]. That reaction has been studied in detail on Rh catalysts [11]. N_2O reduction by CO on Rh/Al_2O_3 has been studied by McCabe and Wong [22] and the authors proposed a reaction mechanism, which involves dissociative adsorption of N_2O. They suggested that the observed lower activity for the CO/N_2O reaction compared to the CO/O_2 or CO/NO reactions is caused by slower dissociative adsorption of N_2O relative to O_2 and NO. N_2O dissociation might be the rate-determining step, as was also concluded by some other authors [23].

In the present paper the main results described concern N_2O reduction by hydrogen on several gold-based catalysts (Au/Al_2O_3, Au/TiO_2, $Au/M^IO_x/M^{II}O_x/Al_2O_3$, and $Au/MO_x/Al_2O_3$, with M^I, M^{II}, M = Li, Rb, Mg, Co, Mn, Ce, La, Ti). Additional information was achieved by comparing the behavior of Au/Al_2O_3 and Au/TiO_2 catalysts in the H_2/O_2, N_2O/H_2, and N_2O/CO reactions. The main purpose was to study whether the same factors that are crucial for CO oxidation also hold for N_2O reduction (e.g., gold particle size and oxidic additives). For CO oxidation on multicomponent gold catalysts, $Au/M^IO_x/M^{II}O_x/Al_2O_3$, it has been suggested that M^IO_x (M^I, transition metal) plays an impor-

* Corresponding author.
E-mail address: Nieuwe_B@chem.leidenuniv.nl (B.E. Nieuwenhuys).

0021-9517/$ – see front matter
doi:10.1016/S0021-9517(03)00185-4

tant role in O_2 activation, via a *Mars and Van Krevelen*-type mechanism and $M^{II}O_x$ (M^{II}-alkaline earth metal) stabilizes the gold particle size against sintering [3,24]. A beneficial effect of MO_x addition to Au/Al_2O_3 was also observed for CH_4 oxidation [25]. More recently, our studies were focused on the effect of oxides added to gold-based catalysts on total oxidation of propene [26]. It turned out that the addition of $M^IO_x/M^{II}O_x$ to Au/Al_2O_3 results in a drastic increase in catalytic activity of gold catalysts.

The results for the N_2O/H_2 reaction presented here show that the catalytic activity of Au/Al_2O_3 increases dramatically by the addition of MO_x or $M^IO_x/M^{II}O_x$ (M^I and M^{II}, transition metals or alkali metals). The most active catalysts are $Au/Rb_2O/CeO_x/Al_2O_3$ and $Au/Li_2O/CeO_x/Al_2O_3$.

2. Experimental

2.1. Catalyst preparation

γ-Al_2O_3 (Engelhard Al-4172 P, $S_{BET} = 275 m^2\ g^{-1}$, V_p ca. 2.8 ml g^{-1}) and TiO_2 (Eurotitania 1, $S_{BET} = 37\ m^2\ g^{-1}$) were used as supports. Supported MO_x/Al_2O_3 and $M^IO_x/M^{II}O_x/Al_2O_3$ (with M, M^I, M^{II} as defined above) were prepared via pore volume impregnation. Dried γ-Al_2O_3 was placed in a flask under vacuum. Desired amounts of $M(NO_3)_x \cdot yH_2O$ or $M^I(NO_3)_x \cdot yH_2O$ and $M^{II}(NO_3)_n \cdot mH_2O$ were dissolved in the corresponding quantity of demineralized water and were added at room temperature to the support. The precursor was further dried in air at 80 °C for at least 16 h. Subsequently, the sample was calcined in O_2 flow at 350 °C for 2 h.

Au was added to Al_2O_3, MO_x/Al_2O_3, $M^IO_x/M^{II}O_x/Al_2O_3$, or TiO_2 via homogeneous deposition precipitation (HDP) using urea as precipitating agent [27]. An aqueous solution of $HAuCl_4 \cdot 3H_2O$ (99.999%, Aldrich) was used as gold precursor. The suspension was heated at ca. 70 °C under vigorous stirring in order to decompose the urea. In this way the pH of the solution gradually increased up to 8. The suspension was then cooled, filtered, and washed several times with demineralized water in order to remove chlorine ions. Finally, the samples were dried overnight in air at 80 °C and, subsequently, calcined in O_2 flow at 300 °C for 2 h. The supported gold catalysts had a theoretical Au loading of 5 wt% and an Au:M atomic ratio of 1:5. The intended $Au:M^I:M^{II}$ atomic ratio was 1:5:5 in the case of $Au/M^IO_x/M^{II}O_x/Al_2O_3$.

2.2. Catalyst characterization

The gold loading was verified by atomic absorption spectroscopy (AAS) using a Perkin-Elmer 3100 with an air/acetylene flame. For that purpose, the catalysts were dissolved in aqua regia and the solution was diluted with demineralized water before the analysis was performed.

BET surface areas of the catalysts were measured by N_2 physisorption at −196 °C using an automatic Qsurf M1 analyzer. Before each measurement the catalyst was heated in helium at 200 °C for 2 h in order to remove impurities adsorbed on the surface.

To obtain information about the identity of the metal/oxide phases present on the catalyst, several techniques have been used, including XRD, UV–vis, TEM, and EDX. X-ray diffraction (XRD) was performed using a Philips Goniometer PW 1050/25 diffractometer equipped with a PW Cu 2103/00 X-ray tube operating at 50 kV and 40 mA. The average gold particle size was estimated from XRD line broadening by using the Scherrer equation [28]. The spectra were recorded between $2\theta = 20°$and $2\theta = 60°$.

Diffuse-reflectance UV–vis spectroscopy was conducted with a commercial unit (Perkin-Elmer Spectrometer, Lambda 900) over air-exposed samples. The scan was made between 200 and 2000 nm with a band pass of 1 nm.

Transmission electron microscopy (TEM) was used to examine in more detail the particle size distribution for some of the samples tested. TEM experiments were performed using a Philips CM30UT microscope equipped with a LaB_6 filament as the source of electrons operated at 300 kV. The samples were mounted on a micro-grid carbon polymer supported on a copper grid by placing a few droplets of a suspension of ground catalyst in ethanol on the grid, followed by drying under ambient conditions. Maximum resolution was 0.5 nm at 500k magnification. Elemental analysis was performed using energy dispersive X-ray analysis (EDX).

2.3. Activity measurements

The reduction and oxidation reactions were carried out in a lab-scale fixed-bed reactor in which typically 200 mg catalyst was used. Prior to measurements, the catalysts were either reduced in 4 vol% H_2 or oxidized in 4 vol% O_2, both in He balance, at 300 °C, and kept at that temperature for 30 min. The feed gases were controlled by mass flow controllers (Bronkhorst) and set to a total flow of 30 ml min^{-1}. All the gases were 4 vol% in He and different ratios were used: for $N_2O/CO = 0.5$ and 2, for $N_2O/H_2 = 0.2$ and 0.5, for $CO/O_2 = 2$ and 1, and for $O_2/H_2 = 1$. The reaction was started after stabilization at room temperature for at least 30 min. Most of the experiments were performed in a temperature programmed way: the temperature was slowly increased or decreased (5 °C min^{-1}) between room temperature and 300 °C. The temperature ramp of 5 °C min^{-1} was considered to be sufficiently slow to reach at every point a pseudo-steady state. Each experiment consisted of two heating cycles and two cooling cycles, in order to monitor possible hysteresis and catalyst deactivation processes. The effluent stream of the N_2O/H_2 reaction was analyzed by a quadrupole mass spectrometer (Balzers) by monitoring every minute the m/e values of 44 (N_2O), 32 (O_2), 30 (NO), 28 (N_2), 18 (H_2O), and 17 (NH_3). Fragments of N_2O and H_2 interfere with the signals of NO, N_2, and NH_3 and the

Table 1
Fragmentation factors applied for N_2O/H_2 reaction

Gas	Fragment	Interfering with	F
N_2O	NO	NO	0.68
N_2O	N_2	N_2	0.27
H_2O	OH	NH_3	0.27

F (fragmentation factor) = relative signal ratio to original gas.

fragmentation factors listed in Table 1 were used for corrections. These factors were calibrated by using pure gas N_2O in helium and for the water signal its signal intensity measured at a conversion of 100% for the N_2O/H_2 reaction over a Pt/Al_2O_3 catalyst was used. In addition to these corrections, subtraction of the background signal was applied. The N_2O/CO, H_2/O_2, and CO/O_2 reactions were monitored by using a gas chromatograph (GC-2002, Chrompack) equipped with a Molsieve 5 Å column, capable of detecting CO, NO, H_2, O_2, and N_2 and a Haysep A column, capable of detecting CO_2. The effluent flow was analyzed every minute.

3. Results and discussion

3.1. Catalyst characterization

AAS measurements show that the catalyst preparation method resulted in a gold loading close to the target loading of 5 wt% (see Table 2). In the same table are also quoted the surface areas of the samples determined by BET. For most of the catalysts these values did not differ significantly from those of the bare supports (275 $m^2\,g^{-1}$ for γ-Al_2O_3 and 37 $m^2\,g^{-1}$ for Eurotitania).

To identify crystalline phases present in the catalysts, XRD analysis was performed. All the samples showed the diffraction peaks that correspond to metallic gold. For several catalysts the diffraction lines corresponding to the metal oxide additives were found. However, for some samples the formal oxidation state of these oxides could not be identified unambiguously. Presumably, these oxides are present as mixture of oxides. From XRD line broadening the average Au particle size was determined (see Table 2). Since the peak width at half-maximum intensity was used to determine the average particle size, smaller crystallites were not taken into consideration. This is the limitation of XRD to estimate the average particle size. In addition, the average crystallite size does not provide any information about the particle size distribution. Table 2 shows the beneficial role of Li oxide on the gold particle size as is demonstrated by comparing the values of d^{a}_{Au} and d^{b}_{Au} of Au/Al_2O_3, $Au/CeO_x/Al_2O_3$, and $Au/CoO_x/Al_2O_3$ with those of $Au/Li_2O/Al_2O_3$, $Au/Li_2O/CeO_x/Al_2O_3$, and $Au/CoO_x/Li_2O/Al_2O_3$. Similar beneficial effects were reported by Grisel et al. [27] and Bethke et al. [29] for alkali-earth metal oxides.

Table 2
Characterization of gold-based catalysts

Sample	Au loading (wt%)	S_{BET} (m^2/g)	d^{a}_{Au} (nm)	d^{b}_{Au} (nm)
Al_2O_3	–	275	–	–
Au/Al_2O_3	4.7	260	4.3 ± 0.1	5.9 ± 07
$Au/MnO_x/Al_2O_3$	4.0	222	1.4 ± 0.3	14.5 ± 0.5
$Au/MgO/Al_2O_3$	4.0	224	4.0 ± 02	7.1 ± 0.6
$Au/MnO_x/MgO/Al_2O_3$	4.5	265	1.1 ± 0.1	8.0 ± 0.6
$Au/CeO_x/Al_2O_3$	4.5	218	2.4 ± 0.4	9.9 ± 0.4
$Au/Li_2O/Al_2O_3$	4.0	278	3.3 ± 0.1	4.0 ± 0.3
$Au/Li_2O/CeO_x/Al_2O_3$	4.6	262	1.9 ± 0.5	7.2 ± 0.6
$Au/CoO_x/Al_2O_3$	4.0	207	3.8 ± 0.1	6.1 ± 0.8
$Au/CoO_x/Li_2O/Al_2O_3$	4.6	247	2.0 ± 0.2	3 ± 0.2
$Au/Rb_2O/Al_2O_3$	4.2	279	7.0 ± 0.5	11.5 ± 0.4
$Au/Rb_2O/CeO_x/Al_2O_3$	4.5	275	1.3 ± 0.3	7.4 ± 0.3
Au/TiO_2	4.9	38	3.9 ± 0.2	6.5 ± 0.1
$Au/TiO_x/Al_2O_3$	4.7	243	1.8 ± 0.1	5.1 ± 0.5

Average size of gold particles for fresh sample d^{a}_{Au} and for spent sample d^{b}_{Au} (XRD measurements).

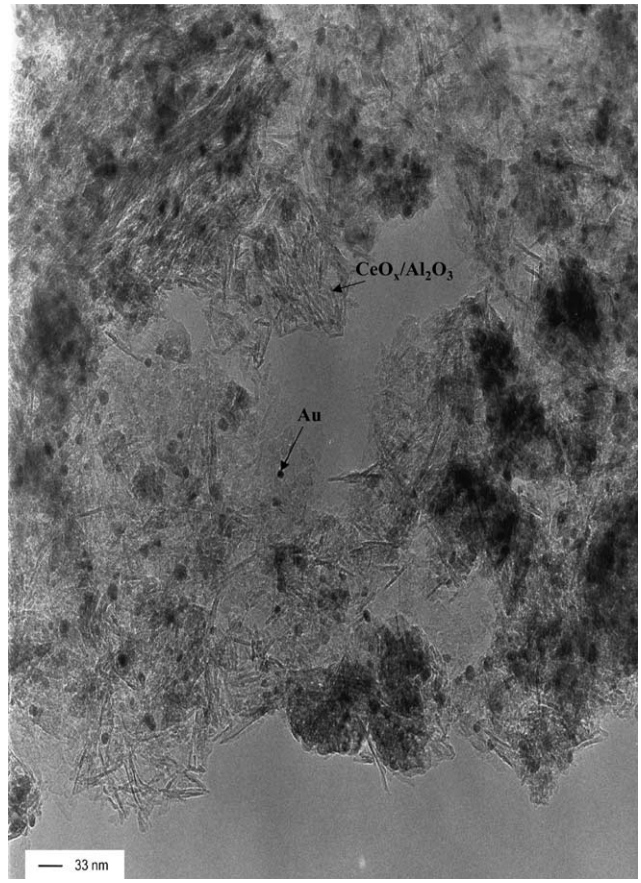

Fig. 1. HRTEM image of $Au/CeO_x/Al_2O_3$.

HRTEM was used to investigate the particle-size distribution. A typical TEM micrograph of the $Au/CeO_x/Al_2O_3$ catalyst is presented in Fig. 1. The gold particles are uniformly distributed on the support, a general characteristic of all the samples studied by HRTEM. Hence, the preparation method used proved to be a suitable one to obtain

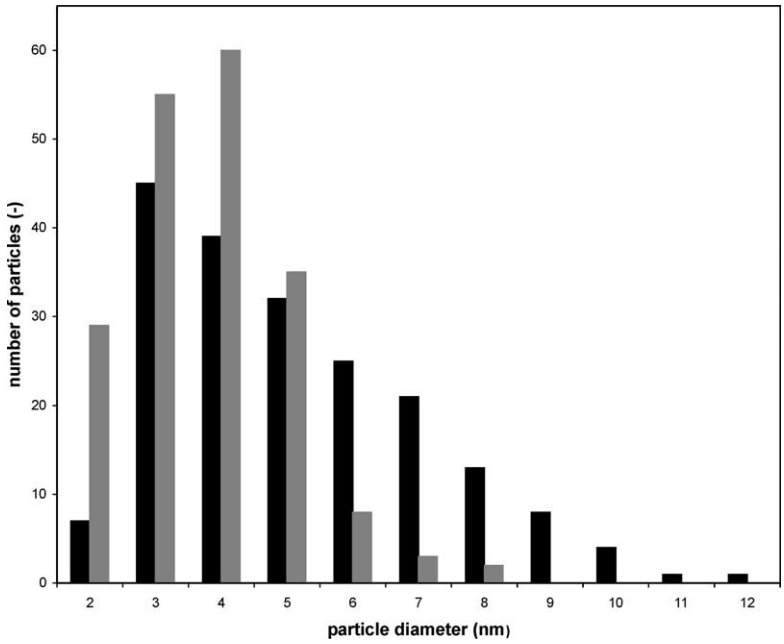

Fig. 2. Size distribution of Au particles supported on CeO_x/Al_2O_3 (black) and $Li_2O/CeO_x/Al_2O_3$ (gray).

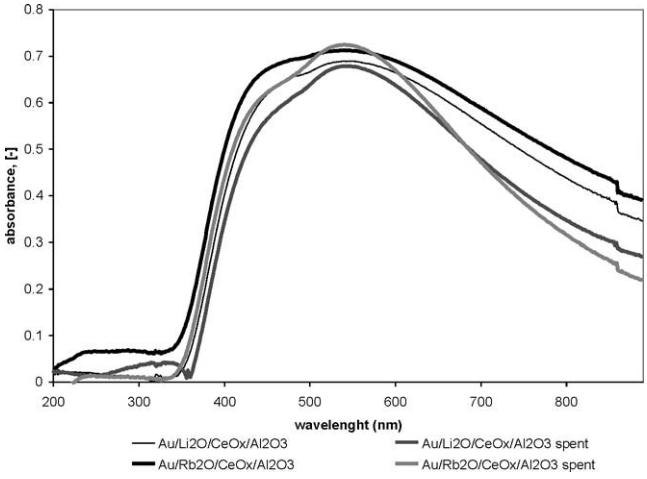

Fig. 3. UV–vis spectra for fresh and spent catalysts (N_2O/H_2 reaction, reactant ratio 0.5).

gold particles uniformly distributed on the oxide support. The mean gold particle size for $Au/CeO_x/Al_2O_3$ was estimated to be ~ 4 nm (HRTEM). The distribution of the particle size for $Au/CeO_x/Al_2O_3$ and $Au/Li_2O/CeO_x/Al_2O_3$, as determined by HRTEM, is shown in Fig. 2. There is a good agreement between the results of XRD and HRTEM measurements.

UV–vis spectra for some selected catalysts are presented in Fig. 3. All the spectra shown were obtained after subtraction of the support contribution. The most prominent feature of these samples is an absorbance band at around 550 nm, which is typically of the plasmon resonance peak of metallic gold [30]. There is no indication that gold is present in an ionic form. The spent catalysts show similar absorbance spectra as the fresh catalysts.

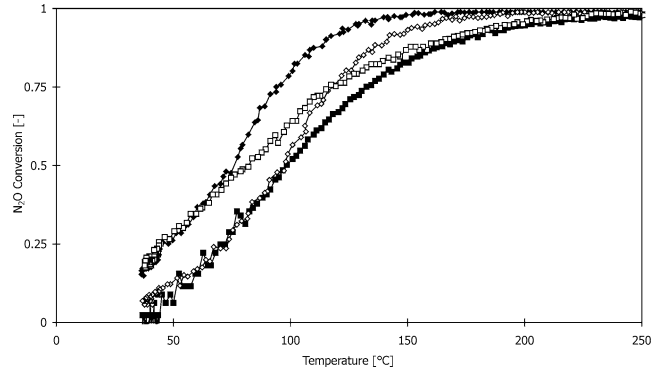

Fig. 4. N_2O reduction versus temperature during N_2O–H_2 reaction over (♦) prereduced Au/TiO_2, (■) prereduced Au/Al_2O_3, (◊) preoxidized Au/TiO_2, and (□) preoxidized Au/Al_2O_3. $N_2O/H_2 = 0.2$.

3.2. Comparative studies of N_2O reduction by hydrogen or CO and H_2 and CO oxidation by O_2 over Au/Al_2O_3 and Au/TiO_2 catalysts

Decomposition of N_2O in the absence of a reducing gas was not observed.

The presentation of the results of N_2O reduction with H_2 will be divided into: (i) N_2O reduction with H_2 on Au/Al_2O_3 and Au/TiO_2 measured following either reductive or oxidative pretreatment using a reactant ratio of 0.2 and (ii) N_2O reduction with hydrogen on $Au/M^IO_x/M^{II}O_x/Al_2O_3$ and $Au/MO_x/Al_2O_3$ (M^I, M^{II}, M = Li, Rb, Mg, Co, Mn, Ce, La, Ti) by using a reactant ratio of 0.5. The latter results will be described in Section 3.3.

The conversion of nitrous oxide over Au/TiO_2 and Au/Al_2O_3 with different pretreatments is depicted in Fig. 4 ($N_2O/H_2 = 0.2$). The figure shows the conversion versus

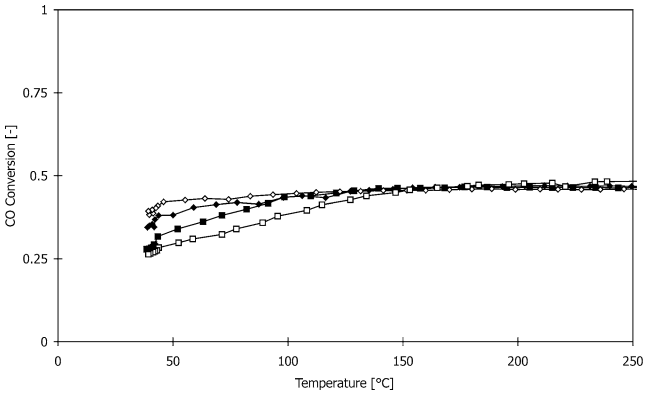

Fig. 5. CO oxidation versus temperature during N_2O–CO reaction over (♦) prereduced Au/TiO_2, (■) prereduced Au/Al_2O_3, (◊) preoxidized Au/TiO_2, and (□) preoxidized Au/Al_2O_3. $N_2O/CO = 0.5$.

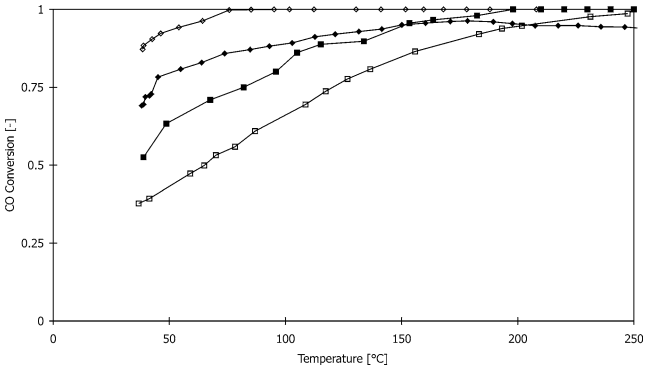

Fig. 6. CO oxidation versus temperature during N_2O–CO reaction over (♦) prereduced Au/TiO_2, (■) prereduced Au/Al_2O_3, (◊) preoxidized Au/TiO_2, and (□) preoxidized Au/Al_2O_3. $N_2O/CO = 2$.

temperature as observed during the cooling stage. However, these results were almost similar to those observed at the heating stage. All the catalysts exhibited a high catalytic activity even at low temperatures. However, differences in behavior of the catalysts were found. In the temperature range between 75 and 175 °C the highest conversion is reached over Au/TiO_2-reductive pretreatment. The only detected products were N_2 and H_2O. NH_3 and NO were not detected.

N_2O/CO reaction has been studied over the same catalysts, using two different reactant ratios, with either an excess of CO ($N_2O/CO = 0.5$) or an excess of N_2O ($N_2O/CO = 2$). The conversion of the samples versus temperature during the cooling stage is presented in Fig. 5 for the N_2O/CO ratio of 0.5 and in Fig. 6 for the ratio 2.

As can be seen from Fig. 5, all the samples are already active at room temperature and full N_2O conversion (as indicated by a CO conversion of 50%) was reached around 100 °C. There are no significant differences between either preoxidized or prereduced samples, or Au/Al_2O_3 and Au/TiO_2.

When excess N_2O was used ($N_2O/CO = 2$), the differences in activity patterns between Au/TiO_2 and Au/Al_2O_3 and oxidative and reductive pretreatment are larger than for $N_2O/CO = 0.5$. The results are depicted in Fig. 6. All the

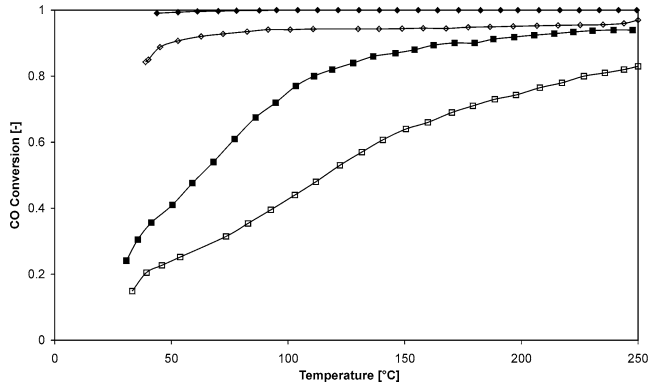

Fig. 7. CO oxidation versus temperature during CO–O_2 reaction over (♦) prereduced Au/TiO_2, (■) prereduced Au/Al_2O_3, (◊) preoxidized Au/TiO_2, and (□) preoxidized Au/Al_2O_3. $CO/O_2 = 2$.

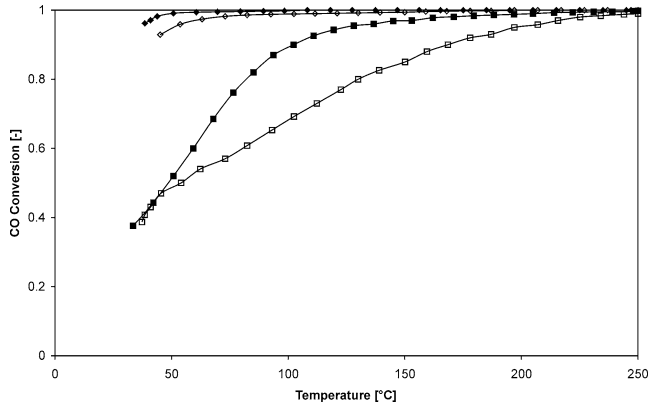

Fig. 8. CO oxidation versus temperature during CO–O_2 reaction over (♦) prereduced Au/TiO_2, (■) prereduced Au/Al_2O_3, (◊) preoxidized Au/TiO_2, and (□) preoxidized Au/Al_2O_3. $CO/O_2 = 1$.

samples were able to fully convert CO at temperatures below 200 °C. The sequence of increasing conversion for the investigated samples was similar to that found for a N_2O/CO ratio of 0.5: preoxidized Au/Al_2O_3 < prereduced Au/Al_2O_3 < prereduced Au/TiO_2 < preoxidized Au/TiO_2. During reaction the only detected products were CO_2 and N_2. NO formation was not observed.

The two types of catalysts used in this comparative study were quite active for CO oxidation by O_2, as shown in Figs. 7 and 8 [31].

Fig. 9 presents the results of the activity experiments for H_2 oxidation with O_2 carried out on the same set of Au/Al_2O_3 and Au/TiO_2 catalysts. The figure shows the hydrogen conversion during the cooling stage; the oxygen conversion follows a similar pattern. The applied H_2/O_2 ratio was 1 (excess oxygen). All the samples are already active at room temperature, but an interesting feature should be noted: whereas there is no significant difference in catalytic performance of Au/TiO_2 and Au/Al_2O_3 following reductive pretreatment in the whole temperature range studied, the difference between the samples after oxidative pretreatment is significant. An oxidative pretreatment applied to Au/TiO_2 causes an important decrease in its capability to convert H_2.

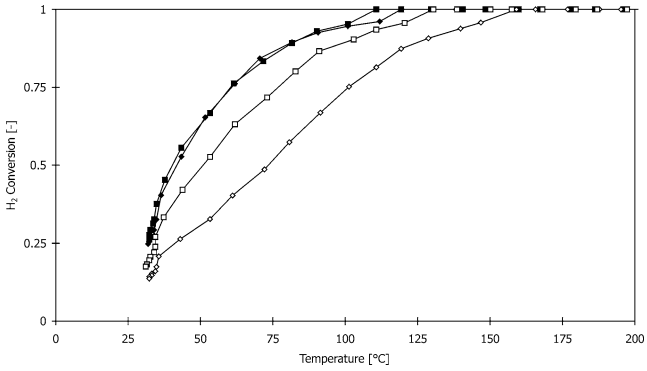

Fig. 9. H_2 oxidation versus temperature during H_2–O_2 reaction over (♦) prereduced Au/TiO_2, (■) prereduced Au/Al_2O_3, (◊) preoxidized Au/TiO_2, and (□) preoxidized Au/Al_2O_3. $H_2/O_2 = 1$.

The general trend is that the TiO_2-supported catalysts are more active than the Al_2O_3-supported ones for the oxidation reactions of CO: $CO + O_2$ and $CO + N_2O$. Interestingly, however, the Al_2O_3-supported preoxidized catalysts exhibit a better performance than the TiO_2-supported preoxidized catalysts for the $H_2 + O_2$ reaction. For the $H_2 + N_2O$ reaction the differences in behavior of the TiO_2 and Al_2O_3-supported catalysts are relatively small.

Prereduced Al_2O_3-supported catalysts are significantly more active than the preoxidized ones. For the TiO_2-supported catalysts the effect of pretreatment is smaller.

It should be noted that the effect of pretreatment is observed for several subsequent runs. However, after many runs (> 5) the effect of pretreatment disappears and the performance of the catalyst shows a behavior intermediate of that of the prereduced and preoxidized catalyst depending on the reactant ratio used.

A summary of $T_{50\%}$ (temperature needed for a conversion of 50%) for all the reactions discussed above is presented in Table 3.

Although a large number of studies dealing with gold catalysis have been reported recently, the nature of active sites and the reaction mechanisms still remain unclear. However, several mechanisms have been proposed in the literature, in an attempt to shed more light on catalysis by gold. Suggestions include a special role of sites at the metal-support interface [14,32,33], the availability of low coordinated surface atoms [34], and quantum size effects [35]. It also has been suggested that an active ensemble of Au–OH and metallic Au atoms may play a key role [36 and the references therein]. Density functional theory calculations point to the role of special reaction geometries available at nanosized gold particles in combination with an enhanced ability of low coordinated gold atoms to interact with molecules from the surroundings. O_2 dissociation appears to be extremely facile on these gold nanoparticles [37]. However, DFT calculations by Liu et al. suggest that O_2 dissociation on gold-particles cannot occur and that the oxidation reactions occur directly via O_2 [38]. In the opinion of the present authors, the mechanism on gold-based catalysts may be similar to that on the platinum group metal (PGM) catalysts [11]. In this light the elementary steps for CO oxidation are

$$CO \rightarrow CO_{ads}, \tag{1}$$

$$O_2 \rightarrow 2O_{ads}, \tag{2}$$

$$O_{ads} + CO_{ads} \rightarrow CO_2, \tag{3}$$

and for the H_2/O_2 reaction [41]:

$$H_2 \rightarrow 2H_{ads}, \tag{4}$$

$$O_2 \rightarrow 2O_{ads}, \tag{5}$$

$$2H_{ads} + O_{ads} \rightarrow H_2O \text{ (via OH ads)}. \tag{6}$$

In this view, gold nanoparticles have the ability to dissociate O_2 and because of its low heat of adsorption, adsorbed oxygen will be very reactive. Hydrogen is not dissociatively adsorbed on gold bulk surfaces [39] especially at low temperatures, but the dissociation might proceed on gold nanoparticles. Some recent results obtained in our laboratory support this proposal. It was found that the rate of the hydrogen–deuterium exchange reaction,

$$H_2 + D_2 \rightleftharpoons 2HD, \tag{7}$$

is much faster over Au/Al_2O_3 catalysts than over Al_2O_3 [40]. The transition metal oxides and ceria may provide an additional route to supply O_{ads} and H_{ads}.

Reduction of N_2O with CO and hydrogen occurs already at room temperature, both Au/Al_2O_3 and Au/TiO_2 exhibiting high catalytic activity. Since only N_2 is formed as a

Table 3
Comparison of the performance of Au/Al_2O_3 and Au/TiO_2 catalysts for the four reactions described in this paper

Reaction	Ratio	$T_{50\%}$ (°C) Au/Al_2O_3		$T_{50\%}$ (°C) Au/TiO_2	
		Preoxidized	Prereduced	Preoxidized	Prereduced
$CO + O_2$	2	100	60	<20	<20
	1	60	50	<20	<20
$H_2 + O_2$	1	40	40	60	70
$CO + N_2O$	2	<50	<50	<50	<50
	0.5	66	<50	<50	<50
$H_2 + N_2O$	5	100	80	80	100
	2	110		80	

nitrogen-containing product, the reduction of N_2O with CO and hydrogen may proceed via a Langmuir–Hinshelwood mechanism, between O_{ads} formed as a result of N_2O dissociation and CO_{ads} or H_{ads} on gold:

$$N_2O \rightarrow N_2O_{ads}, \tag{8}$$

$$N_2O_{ads} \rightarrow N_2 + O_{ads}, \tag{9}$$

$$CO \rightarrow CO_{ads}; \tag{10}$$

or

$$H_2 \rightarrow 2H_{ads}, \tag{11}$$

$$O_{ads} + CO_{ads} \rightarrow CO_2; \tag{12}$$

or

$$2H_{ads} + O_{ads} \rightarrow H_2O. \tag{13}$$

Additional experiments were carried out on Au/Al_2O_3 and Au/TiO_2 in order to detect possible N_2O decomposition in absence of CO or H_2. Without CO or hydrogen in the system, decomposition of N_2O was not observed. Possible reasons may include a buildup of oxygen atoms on the surface that inhibit the reaction [41,42], or the absence of a promoting effect of CO and H_2 on the dissociation of N_2O. The Au–N_2O bond is very weak and desorption proceeds rapidly.

3.3. N_2O reduction with H_2 over multicomponent catalysts

For the applied ratio N_2O/H_2 0.5 several gold-based catalysts were tested and the effect of different additives was studied. The catalytic activities of some selected catalysts are shown in Fig. 10, where the conversion observed at the first cooling branch is depicted. During the other stages the conversion patterns were similar. Difference in $T_{50\%}$ during heating and cooling stages did not exceed 30 °C.

Fig. 10 shows the performance of various gold-based catalysts, viz. Au/Al_2O_3, $Au/CeO_x/Al_2O_3$, $Au/CoO_x/Al_2O_3$, $Au/Li_2O/Al_2O_3$, $Au/Li_2O/CeO_x/Al_2O_3$, and $Au/CoO_x/Li_2O/Al_2O_3$, tested in a $N_2O/H_2 = 0.5$ reaction. Clearly, a large synergistic effect is observed for the multicomponent catalysts. In the temperature range studied (up to 265 °C) the supports did not reveal N_2O conversion higher than 5%. Hence, the measured catalytic activity is due to the presence of gold and not because of the intrinsic activity of the support itself.

All the data regarding $T_{50\%}$ and $T_{95\%}$ conversion for the various catalysts are summarized in Table 4.

N_2O is a thermodynamically unstable molecule. However, the thermal decomposition reaction under homogeneous conditions does occur only above 600 °C. Over gold-based catalysts, experiments of N_2O in the absence of any reducing gas in the system did not reveal any decomposition products. Supported gold catalysts convert nitric oxide in the presence of hydrogen to the following products: N_2O (at low temperature), N_2 (at intermediate temperature), and NH_3 (at high temperature) [31,43]. It was already pointed out before that N_2O reduction with hydrogen produces N_2 as the only nitrogen-containing product. The N–N bonding (474 kJ mol^{-1}) in the N_2O molecule is much stronger than that of N–O (161 kJ mol^{-1}). Therefore, if a N_2O molecule dissociates, a reasonable assumption is that it will break through its N–O bond (14), rather than dissociation to NO_{ads} and N_{ads} (15) [41]:

$$N_2O \rightarrow N_2 + O_{ads}, \tag{14}$$

$$N_2O \rightarrow NO_{ads} + N_{ads}. \tag{15}$$

The adsorbed oxygen then reacts with hydrogen to form water. The experimental results obtained for the H_2/O_2 reaction support this mechanism. Since decomposition of N_2O in the absence of H_2 did not reveal any product formation, it is proposed that the presence of hydrogen enhances the decomposition of nitrous oxide.

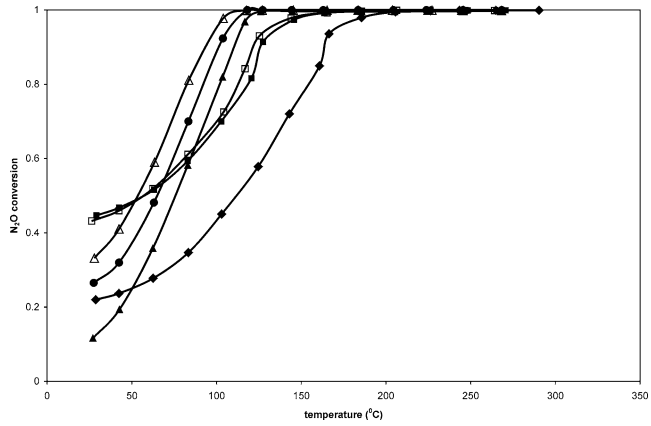

Fig. 10. N_2O reduction versus temperature during N_2O–H_2 reaction over (♦) Au/Al_2O_3, (■) $Au/CeO_x/Al_2O_3$, (▲) $Au/Li_2O/Al_2O_3$, (△) $Au/Li_2O/CeO_x/Al_2O_3$, (□) $Au/CoO_x/Al_2O_3$, and (●) $Au/CoO_x/Li_2O/Al_2O_3$. $N_2O/H_2 = 0.5$.

Table 4
Catalytic activity of gold-supported catalysts for N_2O/H_2 reaction (reactant ratio $N_2O/H_2 = 0.5$)

Catalyst	$T_{50\%}$ (°C)	$T_{95\%}$ (°C)
Au/Al_2O_3	111	265
$Au/Li_2O/CeO_x/Al_2O_3$	52	122
$Au/Li_2O/Al_2O_3$	75	145
$Au/Rb_2O/CeO_x/Al_2O_3$	50	115
$Au/Rb_2O/Al_2O_3$	160	265
$Au/CeO_x/Al_2O_3$	56	205
$Au/CoO_x/Li_2O/Al_2O_3$	64	118
$Au/CoO_x/Al_2O_3$	57	205
$Au/TiO_2/Al_2O_3$	82	160
$Au/MnO_x/MgO/Al_2O_3$	69	145
$Au/MgO/Al_2O_3$	103	225
$Au/MnO_x/Al_2O_3$	140	265
$Au/La_2O_3/Al_2O_3$	110	206
$Au/MoO_x/Al_2O_3$	179	–
$Li_2O/CeO_x/Al_2O_3$	>265	–

The mechanism of the beneficial effects of the additives (TMO, ceria or alkali metal oxides) is still under debate. Many researchers agree that the gold–TMO interface may play a significant role [10,33,39,44]. The present results prove that reduction of N_2O to N_2 and O_{ads} is enhanced in the presence of a TMO or ceria, or, more general, oxides with a high capability to store and release oxygen (see Fig. 10). The presence of CeO_x or a TMO might create new sites for N_2O dissociation at the gold/ceria or TMO interface. A striking result is that by addition of both an alkali metal oxide (Li_2O or Rb_2O) and CeO_x or a TMO, a dramatic increase in the catalyst performance is obtained. This can be explained by taking into consideration the already discussed effect of ceria on catalytic activity, in combination with the beneficial effect of an (earth) alkali metal oxide on the performance of gold-catalysts. The basicity of the alkali metal oxide increases from Li_2O to Rb_2O. To the best of our knowledge, this is the first time that such a large synergistic effect was found for gold catalysts by adding both an alkali metal oxide and a transition metal oxide. The effect of alkali or alkali–earth metal oxide on Pt/Al_2O_3 was extensively studied by Yentekakis and co-workers [45–47] for NO reduction by propene in the presence of oxygen. In case of Pt/Al_2O_3, the promoting effect of Rb_2O is the biggest one. The effect of basicity on the catalytic activity was also observed in a hydrogen/water isotopic exchange reaction on nickel-based catalysts [48]. For gold-supported catalysts, the combined actions of Rb_2O (Li_2O) and CeO_x are very efficient: sintering of gold particles is prevented by the presence of the promoter Rb_2O (Li_2O) and the intrinsic catalytic activity is enhanced by the presence of the cocatalyst CeO_x. The lower catalytic activity of $Au/Rb_2O/Al_2O_3$ compared with $Au/Li_2O/Al_2O_3$ can be explained by the difference in mean diameter of gold particles (as shown by XRD and HRTEM) of these two samples.

A significant synergistic effect is also found for multicomponent catalysts containing both an alkali metal oxide and a TMO, in this case CoO_x (Fig. 10). However, the enhancement in activity is not as big as in the case of ceria and an alkali metal oxide.

Table 3 also presents another set of three catalysts, viz. $Au/MnO_x/Al_2O_3$, $Au/MgO/Al_2O_3$, and $Au/MnO_x/MgO/Al_2O_3$. As expected, a synergistic effect is again observed. The slightly lower conversion of N_2O on this catalyst compared with the multicomponent $Au/CeO_x/Rb_2O/Al_2O_3$ can be twofold: MgO's basicity and the redox cycle which involves MnO_x. However, $Au/MnO_x/MgO/Al_2O_3$ was found to be very efficient also in total CO oxidation and selective oxidation of CO in hydrogen atmosphere [3].

4. Conclusions

Gold-based catalysts are active at low temperature for N_2O/CO, H_2/O_2, CO/O_2, and N_2O/H_2 reactions. The nature of the additives is crucial to obtain a good performance in reduction of nitrous oxide with hydrogen or carbon monoxide and in carbon monoxide oxidation, but is not so important for hydrogen oxidation. The active catalysts mainly contain gold in the metallic form.

During N_2O reduction with H_2 or CO the only products obtained are N_2 and H_2O or CO_2, respectively. It is suggested that the role of the partly reducible metal oxide additive is to contribute to the formation of new active sites and increase N_2O dissociation. On the other hand, alkali or alkali-earth metal oxides stabilize gold particles against sintering. An increasing basicity results in an increased promoting effect.

Acknowledgments

The authors thank Dr. P.J. Kooyman of the National Centre for High Resolution Electron Microscopy, Delft University of Technology, Delft, The Netherlands, for performing the HRTEM measurements. This work has been performed under the auspices of NIOK, the Netherlands Institute for Catalysis Research.

References

[1] M. Haruta, CATTECH 6 (2002) 102.
[2] G.C. Bond, D. Thompson, Gold Bull. 33 (2000) 41.
[3] R.J.H. Grisel, K.J. Weststrate, A.C. Gluhoi, B.E. Nieuwenhuys, Gold Bull. 35 (2002) 39.
[4] M. Haruta, N. Yamada, T. Kobayashi, S. Iijima, J. Catal. 115 (1989) 301.
[5] M. Haruta, T. Kobayashi, H. Sano, N. Yamada, Chem. Lett. 405 (1987).
[6] H. Sakurai, A. Ueda, T. Kobayashi, M. Haruta, J. Chem. Soc., Chem. Commun. (1997) 271.
[7] D. Andreeva, V. Idakiev, T. Tabakova, A. Andreev, J. Catal. 158 (1996) 354.
[8] P. Claus, A. Brückner, C. Mohr, M. Hofmeister, J. Am. Chem. Soc. 122 (2000) 11430.
[9] C. Mohr, M. Hofmeister, M. Lucas, P. Claus, Chem. Eng. Technol. 23 (2000) 4.
[10] M. Haruta, Catal. Surv. Jpn. 1 (1997) 61.
[11] B.E. Nieuwenhuys, Adv. Catal. 44 (1999), and references therein.
[12] M. Haruta, S. Tsubota, T. Kobayashi, H. Kageyama, M. Genet, B. Delmon, J. Catal. 144 (1993) 175.
[13] M. Haruta, N. Yamada, T. Kobayashi, S. Iijima, J. Catal. 115 (1989) 301.
[14] S.D. Lin, M. Bollinger, M. Vannice, Catal. Lett. 17 (1993) 245.
[15] G. Srinivas, J. Wright, C. Bai, R. Cook, Stud. Surf. Sci. Catal. 101 (1996) 427.
[16] A. Ueda, T. Oshima, M. Haruta, Appl. Catal. B 12 (1997) 81.
[17] T. Salama, R. Osnishi, T. Shido, M. Ichikawa, J. Catal. 162 (1996) 169.
[18] T. Salama, R. Ohnishi, M. Ichikawa, Chem. Commun. (1997) 105.
[19] M.A.P. Dekkers, M.J. Lippits, B.E. Nieuwenhuys, Catal. Today 54 (1999) 381.
[20] T. Salama, R. Ohnishi, M. Ichikawa, Faraday Trans. 92 (1996) 301.
[21] N.W. Cant, N. Ossipoff, Catal. Today 36 (1997) 125.
[22] R.W. McCabe, C. Wong, J. Catal. 121 (1990) 422.
[23] D.N. Belton, S.J. Schmeig, J. Catal. 144 (1993) 9.
[24] R.J.H. Grisel, B.E. Nieuwenhuys, J. Catal. 199 (2001) 48.

[25] R.J.H. Grisel, J.J. Slyconish, B.E. Nieuwenhuys, Top. Catal. 1–4 (2001) 425.
[26] A.C. Gluhoi, B.E. Nieuwenhuys, N. Bogdanchikova, to be published.
[27] R.J.H. Grisel, P.J. Kooyman, B.E. Nieuwenhuys, J. Catal. 191 (2000) 430.
[28] P. Scherrer, Nachr. K. Ges. Wiss., Göttingen (1918) 98.
[29] G.K. Bethke, H.H. Kung, Appl. Catal. A 194 (2000) 43.
[30] Y.S. Su, M.Y. Lee, S.D. Lin, Catal. Lett. 57 (1999) 49.
[31] M.A.P. Dekkers, PhD thesis, Leiden University, 2000.
[32] M. Haruta, Catal. Today 29 (1997) 153.
[33] R.J.H. Grisel, B.E. Nieuwenhuys, Catal. Today 64 (2001) 69.
[34] F. Boccuzzi, G. Cerrato, F. Pinna, G. Strukul, J. Phys. Chem. B 102 (1998) 5733.
[35] M. Valden, X. Lai, D.W. Goodman, Science 281 (1998) 1647.
[36] C.K. Cosello, J.H. Yang, H.-Y. Law, Y. Wang, J.-N. Lin, L.D. Marks, M.C. Kung, H.H. Kung, Appl. Catal. A 243 (2003) 15.
[37] N. Lopez, J.K. Norskov, J. Am. Chem. Soc. 124 (2002) 11262.
[38] Z.-P. Liu, P. Hu, A. Alavi, J. Am. Chem. Soc. 124 (2002) 14770.
[39] B.E. Nieuwenhuys, in: R.W. Joyner, R.A. van Santen (Eds.), Elementary Reaction Steps in Heterogeneous Catalysis, Kluwer Academic, Dordrecht, 1993, p. 155.
[40] H.S. Vreeburg, J.W. Bakker, B.E. Nieuwenhuys, to be published.
[41] S.A. Carabineiro, B.E. Nieuwenhuys, Surf. Sci. 495 (2001) 1.
[42] J. Ma, N.M. Rodriguez, M.A. Vannice, R.T.K. Baker, Top. Catal. 10 (2000) 27.
[43] A.C. Gluhoi, B.E. Nieuwenhuys, to be published.
[44] R.J.H. Grisel, C.J. Weststrate, A. Goosens, M.W.J. Craje, A.M. van der Kraan, B.E. Nieuwenhuys, Catal. Today 72 (2002) 223.
[45] I.V. Yentekakis, M. Konsolakis, R.M. Lambert, N. Macleod, L. Nalbantian, Appl. Catal. B 22 (1999) 123.
[46] M. Konsolakis, I.V. Yentekakis, J. Catal. 198 (2001) 142.
[47] M. Konsolakis, I.V. Yentekakis, Appl. Catal. B 29 (2001) 103.
[48] A.C. Gluhoi, P. Marginean, D. Lupu, E. Indrea, A.R. Biris, Appl. Catal. A 232 (2002) 121.